

Thermodynamic Properties of Coquimbite and Aluminocoquimbite

Yu. D. Gritsenko^{a, b, *}, L. P. Ogorodova^{a, **}, M. F. Vigasina^a, D. A. Kosova^c,
S. K. Dedushenko^d, L. V. Melchakova^a, and D. A. Ksenofontov^a

^a Geological Faculty, Lomonosov Moscow State University, Moscow, 119991 Russia

^b Fersman Mineralogical Museum, Russian Academy of Sciences, Moscow, 119692 Russia

^c Chemical Faculty, Lomonosov Moscow State University, Moscow, 119991 Russia

^d NUST MISIS, Moscow, 119049 Russia

*e-mail: ygritsenko@rambler.ru

**e-mail: logor48@mail.ru

Received September 21, 2022; revised November 7, 2022; accepted November 9, 2022

Abstract—Coquimbite $\text{AlFe}_3^{3+} [\text{SO}_4]_6(\text{H}_2\text{O})_{12} \cdot 6\text{H}_2\text{O}$ (sample from the Javier Mine, Peru) has been studied by thermal and electron microprobe analysis, X-ray powder diffraction, Raman spectroscopy, and Mössbauer spectroscopy. The enthalpy of formation of the coquimbite from elements $\Delta_f H^0(298.15 \text{ K}) = -11118 \pm 40 \text{ kJ/mol}$ was determined by the method of solution calorimetry in melt of lead borate $2\text{PbO} \cdot \text{B}_2\text{O}_3$ on a Setaram (France) Calvet microcalorimeter. The value of its absolute entropy $S^0(298.15 \text{ K}) = 1248.3 \pm 3.0 \text{ J/(mol} \times \text{K)}$ was estimated, the entropy of formation $\Delta_f S^0(298.15 \text{ K}) = -5714.0 \pm 3.0 \text{ J/mol} \times \text{K}$, and the Gibbs energy of formation from elements $\Delta_f G^0(298.15 \text{ K}) = -9411 \pm 40 \text{ kJ/mol}$ were calculated. The values of the enthalpy and Gibbs energy of formation of aluminocoquimbite $\text{Al}_2\text{Fe}_2^{3+} [\text{SO}_4]_6(\text{H}_2\text{O})_{12} \cdot 6\text{H}_2\text{O}$ from elements were estimated at -11540 ± 29 and $-9830 \pm 29 \text{ kJ/mol}$, respectively.

Keywords: coquimbite, X-ray powder diffraction, Raman spectroscopy, Mössbauer spectroscopy, thermal analysis, Calvet microcalorimetry, enthalpy, entropy, Gibbs energy

DOI: 10.1134/S0016702923050051

INTRODUCTION

Aluminocoquimbite, paracoquimbite, and aluminocoquimbite are secondary minerals found in arid regions in the oxidation zones of sulfide deposits containing pyrite, marcasite, or pyrrhotite (in Peru, Chile, California and Utah in the United States, Argentine, Australia, Bolivia, China, Mongolia, Greece, Iran, Morocco, Portugal, South Africa, and Spain) and, more rarely, in areas with fumarole volcanic activity (for example, on Shiveluch volcano in Kamchatka, Russia, and Vulcano Island in Italy). Aluminocoquimbite has also been identified by high-sensitivity remote sensing techniques among iron hydrous sulfates on the surface of Mars (Poitras et al., 2018; Turenne et al., 2022).

Coquimbite $\text{AlFe}_3^{3+} [\text{SO}_4]_6(\text{H}_2\text{O})_{12} \cdot 6\text{H}_2\text{O}$ (IMA list of minerals) and paracoquimbite $\text{Fe}_4^{3+} [\text{SO}_4]_6(\text{H}_2\text{O})_{12} \cdot 6\text{H}_2\text{O}$ (IMA list of minerals) crystallize in the trigonal system, space groups $P\bar{3}1c$ and $R\bar{3}$, respectively and are described as polytypes in (Robinson and Fang, 1971). The coquimbite and paracoquimbite structures contain isolated $[\text{Fe}(\text{H}_2\text{O})_6]^{3+}$ and/or $[\text{Al}(\text{H}_2\text{O})_6]^{3+}$ octahedrons and $[\text{Fe}_3(\text{SO}_4)_6(\text{H}_2\text{O})_6]^{3-}$ clusters, in which Fe atoms in one of the sites are coordinated by six oxy-

gens, all of which belong to sulfate ions, and each of the two Fe atoms in the other sites are coordinated by three oxygens of sulfate ions and three oxygens of H_2O molecules. The structures of the minerals involve a complicated system of hydrogen bonds between water molecules of the clusters, isolated octahedrons, and molecules in the interstices (Yang and Giester, 2018). The structure of aluminocoquimbite $\text{Al}_2\text{Fe}_2^{3+} [\text{SO}_4]_6(\text{H}_2\text{O})_{12} \cdot 6\text{H}_2\text{O}$ (IMA list of minerals), which belongs to the trigonal system, space group $P\bar{3}1c$, differs from the coquimbite structure in containing isolated $\text{Al}(\text{H}_2\text{O})_6^{3+}$ octahedrons and infinite $[\text{Fe}(\text{SO}_4)_3]_\infty$ columns on [001], which are made up of octahedrally coordinated Fe atoms and sulfate ions, similar to the ferrinatrite $\text{Na}_3(\text{H}_2\text{O})_3[\text{Fe}(\text{SO}_4)_3]$ structure. The interstitial H_2O molecules are fixed by hydrogen bonds, similar to what occurs in the coquimbite structure (Demartin et al., 2010a, 2010b).

Earlier coquimbite, paracoquimbite, and aluminocoquimbite studies were centered first of all on their structure and on evaluating their unit-cell parameters (Fang and Robinson, 1970; Robinson and Fang, 1971; Majzlan et al., 2010; Yang and Giester, 2018; Mauro

et al., 2020). The IR and Raman spectra of the phases were studied in (Majzlan et al., 2011; Frost et al., 2014; Mauro et al., 2020), and their thermal stability was explored in (Ackermann et al., 2009; Frost et al., 2014).

Applied and academic studies of hydrous iron sulfates, coquimbite among others, were launched in view of the role played by this mineral in the process of weathering of rocks containing relatively much sulfide minerals (which are most commonly, pyrite, marcasite, and/or pyrrhotite), when interactions of water and air with the sulfides result in water-soluble sulfates and sulfuric acid. The latter affects the rocks and enables the leaching of metals (including toxic ones) from these rocks by acidic drainage waters into soil horizons and thus ecologically endangers the agricultural and various other uses of these territories.

The solutions of problems related to environmental pollutions can be facilitated by the theoretical modeling of physicochemical processes in the water–rock systems. This modeling is carried out using thermodynamic data on minerals, with such data sometimes being critically insufficient. For example, we are aware only of a single paper (Majzlan et al., 2006) published so far in which data of acid calorimetry were utilized to determine the enthalpy of formation from elements, evaluate the standard entropy, and calculate the Gibbs energy of coquimbite of the composition $(\text{Fe}_{1.47}^{3+}\text{Al}_{0.53})[\text{SO}_4]_3(\text{H}_2\text{O})_{9.65}$. Hemingway et al. (2002) present only rough estimates of the main thermodynamic parameters of paracoquimbite of the composition $\text{Fe}_2^{3+}[\text{SO}_4]_3 \cdot 9\text{H}_2\text{O}$, which is regarded in this publication as coquimbite. Ackermann et al. (2009) applied acid calorimetry to determine the enthalpy of formation of synthetic analogue of paracoquimbite.

Our study was aimed at the experimental determination of the enthalpy of formation of coquimbite from elements by the method of melt solution calorimetry.

EXPERIMENTAL

Materials and Methods

Our study was carried out with a coquimbite sample (no. 98041) provided for this study by Fersman Mineralogical Museum, Russian Academy of Sciences. The sample originates from the Javier Mine in Peru and is a subparallel aggregate (so-called *brush*) of transparent deep lavender-colored crystals up to 3 mm tall on a fine-grained carbonate rock.

The **X-ray powder diffraction (XRD) study** was carried out on a STOE-STADI MP (Germany) diffractometer with a curved Ge (III) monochromator, which yields strictly monochromatic $\text{CoK}\alpha_1$ radiation ($\lambda = 1.78897\text{\AA}$). The data are acquired by successively

covering scan regions using a position-sensitive linear detector (capture 2Θ angle 5° and 0.02° channel).

The spectrum (Fig. 1) corresponds to that of coquimbite (from Peru) according to ICDD (International Centre for Diffraction Data, 2013; card no. 01-071-2380) data.

The **thermal behavior** of the mineral from room temperature to $T = 673\text{ K}$ was studied on a NETZSCH TG 209 F1 (Germany) thermogravimetric analyzer in nitrogen flow ($40\text{ mL} \times \text{min}^{-1}$) at a heating rate of $10\text{ K} \times \text{min}^{-1}$. The tool was calibrated on the melting points of standards provided by the manufacturer (these were Ag, Al, Bi, In, and Sn 99.999% pure). The measurements were conducted in conventionally used aluminum containers with punctured lids. The mass of the sample was 14.70 mg.

The thermogravimetric curve (Fig. 2) shows evidence of mass loss because of the dehydration of the mineral in two stages: first, at 348 to 424 K, with a maximum of $\sim 448\text{ K}$, the mass losses were 9.4%, which corresponds to the release of six H_2O molecules; and, second, the remaining water is released (19.6% mass loss, which corresponds to 12 water molecules) at a maximum of $\sim 453\text{ K}$ and terminating at $T = 648\text{ K}$.

The **chemical analysis** was carried out on a JSM-6480LV (Jeol Ltd., Japan) scanning electron microscope (SEM) equipped with an X-Max-50 (Oxford Instruments Ltd., Great Britain), energy-dispersive spectrometer (EDS) at an accelerating voltage of 20 kV and current of $10.05 \pm 0.05\text{ nA}$. The raw data were processed with the INCA (Oxford Instruments, v. 22) software.

According to microprobe and thermogravimetric data, the composition (wt %) of the mineral is as follows: Na_2O 0.08, K_2O 0.7, Al_2O_3 4.36, Fe_2O_3 21.58, SO_3 43.19, and H_2O 29.00. The formula of the mineral was calculated by normalizing to twelve charges and is $\text{Al}_{0.97}\text{Fe}_{3.04}^{3+}\text{Na}_{0.03}\text{K}_{0.02}[\text{SO}_4]_{6.04}(\text{H}_2\text{O})_{12} \cdot 6\text{H}_2\text{O}$, which is close to the IMA-recommended theoretical formula $\text{AlFe}_3^{3+}[\text{SO}_4]_6(\text{H}_2\text{O})_{12} \cdot 6\text{H}_2\text{O}$.

The **gamma-resonance study** of the coquimbite was carried out on a YaGRS-6 (Persei, Russia) Mössbauer spectrometer at room temperature, with the use of a 8 mCi ^{57}Co source in a Rh matrix. The spectrometer was calibrated using a conventional α -Fe reference target. The spectra were modeled with the HappySloth software (www.happysloth.ru).

The acquired spectrum (Fig. 3) is consistent with the coquimbite spectrum presented in (Dyar et al., 2013) and is reasonably well described by a single widened Lorentz line with ${}^{\text{RT}}\text{IS}_{\alpha-\text{Fe}} = 0.46 \pm 0.01\text{ mm} \times \text{s}^{-1}$, $\text{FWHM} = 0.85 \pm 0.05\text{ mm} \times \text{s}^{-1}$, and $\chi^2 = 1.2$. The measured isomer shift corresponds to the range of values commonly yielded by octahedral oxygen polyhedrons of trivalent iron $[\text{Fe}^{3+}\text{O}_6]$ and is slightly higher

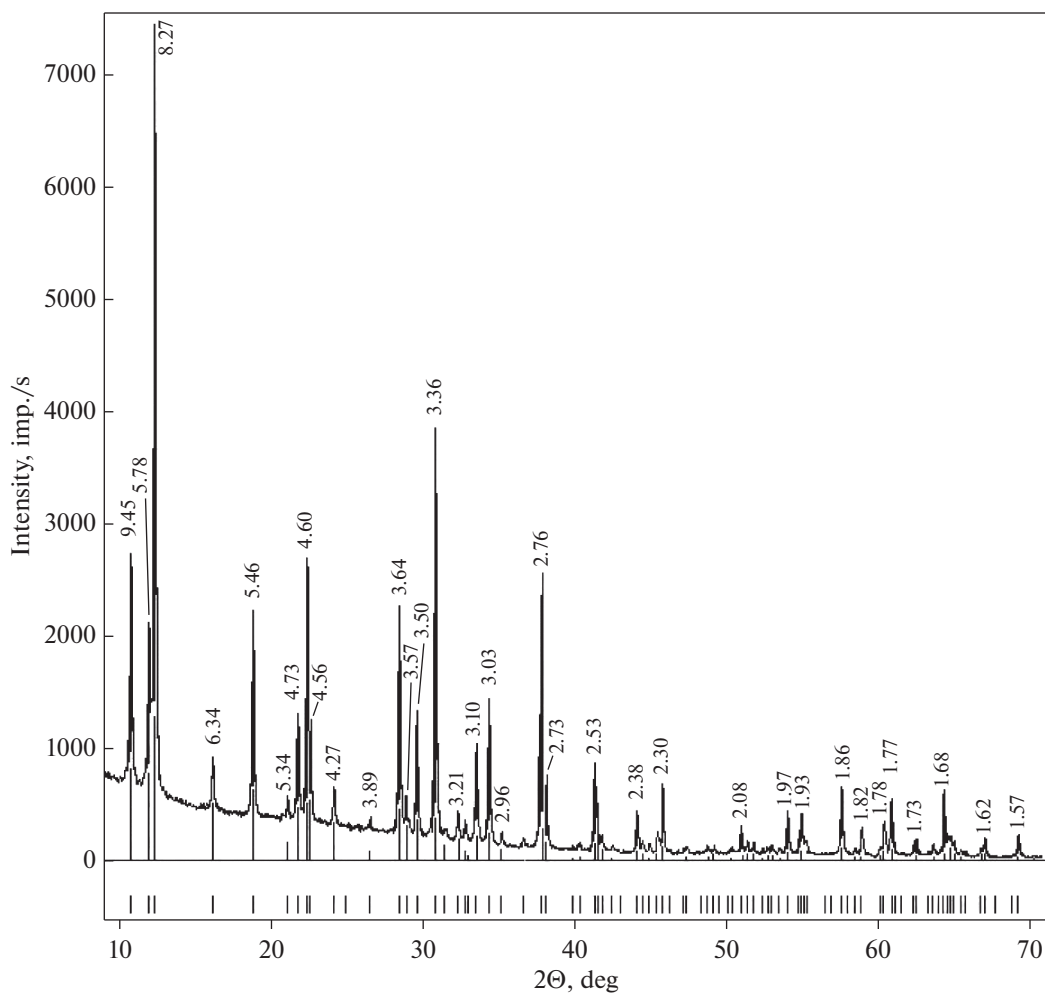


Fig. 1. X-ray powder diffraction pattern of the coquimbite. Interplanar spacing values are in Å. The line below the diffractin pattern presents data on coquimbite from ICDD (card no. 01-071-2380).

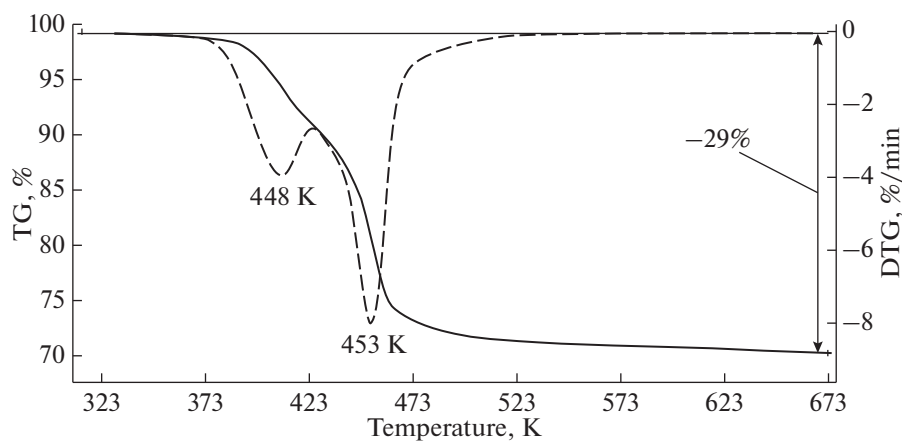


Fig. 2. Thermogravimetric heating curves of the coquimbite.

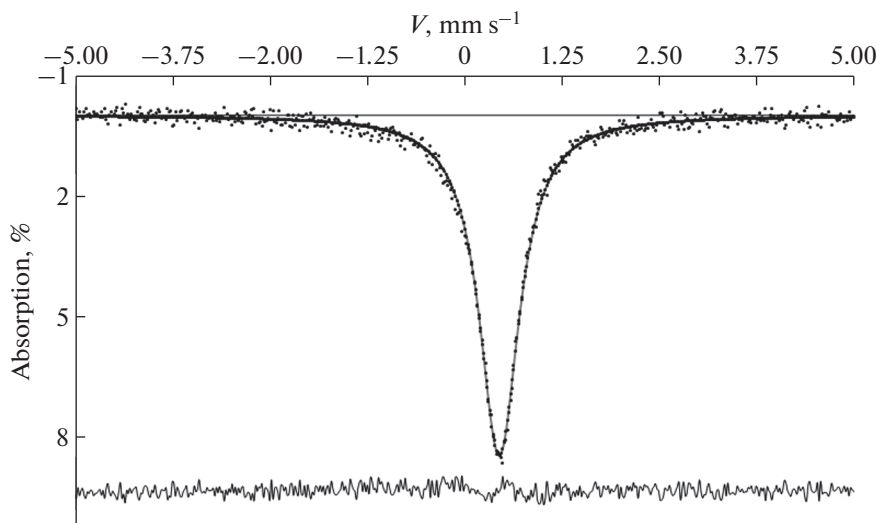


Fig. 3. Room-temperature Mössbauer spectrum of the coquimbite.

than the calculated value (Dedushenko and Perfiliev, 2022). This may likely be explained by the polarizing effect of S^{6+} . More detailed interpretations of the spectrum require additional studies at low temperatures.

The **Raman spectroscopic** study was conducted on an EnSpectr R532 (Russia) Raman microscope. The laser wavelength was 532 nm, the output power was 20 mW, the holographic dispersion grating had 1800 grooves per mm, the spectral resolution was approximately 6 cm^{-1} , and the focal spot at a $40\times$ magnification was $7 \mu\text{m}$. The spectrum was recorded within the range of 100 to 4000 cm^{-1} from a disoriented sample, in a mode of signal accumulation for 1 s at averaging over 50 exposures.

The Raman spectrum obtained from the coquimbite (Fig. 4) is consistent with the spectra of this mineral published in (Frost et al., 2014; Mauro et al., 2020). The spectral region of 2800 to 3600 cm^{-1} corresponds to valence vibrations of the hydroxyl groups of water molecules; the range of 1000–1250 cm^{-1} includes lines pertaining to symmetric (the strongest line at 1024 cm^{-1}) and antisymmetric valence vibrations of $[\text{SO}_4]^{2-}$ -tetrahedrons; the deformation vibrations of SO_4 tetrahedrons yield lines within the region of 440–630 cm^{-1} ; and the spectral region below 300 cm^{-1} includes lines of the scattering of so-called lattice modes (Fe–O and Al–O valence vibrations).

The **thermochemical study** was carried out using a Setaram (France) Tian–Calvet heat-flux microcalorimeter. The enthalpy of formation of the coquimbite was determined by solution calorimetry in $2\text{PbO}\bullet\text{B}_2\text{O}_3$ melt. The solution experiments were carried out as follows: the samples $4\text{--}9$ ($\pm 2 \times 10^{-3}$) mg were dropped from room temperature to the calorimeter with melt at $T = 973 \text{ K}$. The thermal effect involved an increment in the enthalpy of the sample [$(H^0(973 \text{ K}) - H^0(298.15 \text{ K}))$

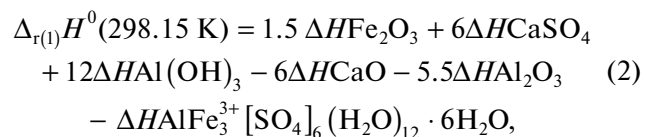
and its dissolution enthalpy $\Delta_{\text{dissol}}H^0(973 \text{ K})$. The ratio of the solute to solvent at six to eight experiments with the same melt portion (30–35 g) is reasonably accurately approximated by infinitely diluted solution with negligibly small mixing enthalpy. The microcalorimeter was calibrated by dropping a standard reference sample (it was platinum) into the melt at the conditions of the dissolution experiments, and therewith only the enthalpy increment [$(H^0(973 \text{ K}) - H^0(298.15 \text{ K}))$] was measured. The required tabulated thermodynamic data were compiled from (Robie and Hemingway, 1995).

The average [$H^0(973 \text{ K}) - H^0(298.15 \text{ K}) + \Delta_{\text{dissol}}H^0(973 \text{ K})$] of seven experiments in the Calvet microcalorimeter, with the natural coquimbite sample was $1312.2 \pm 7.3 \text{ J/g} = 1437.1 \pm 8.0 \text{ kJ/mol}$ ($M = 1095.18 \text{ g/mol}$), the errors were determined at 95% probability.

RESULTS OF THE CHEMICAL STUDY

Enthalpy of Formation from Elements

Using the calorimetric data and thermochemical cycle, which involved the dissolution of the mineral and its components, the enthalpy of formation of the coquimbite from elements was calculated by reaction (1) and Eqs. (2) and (3)



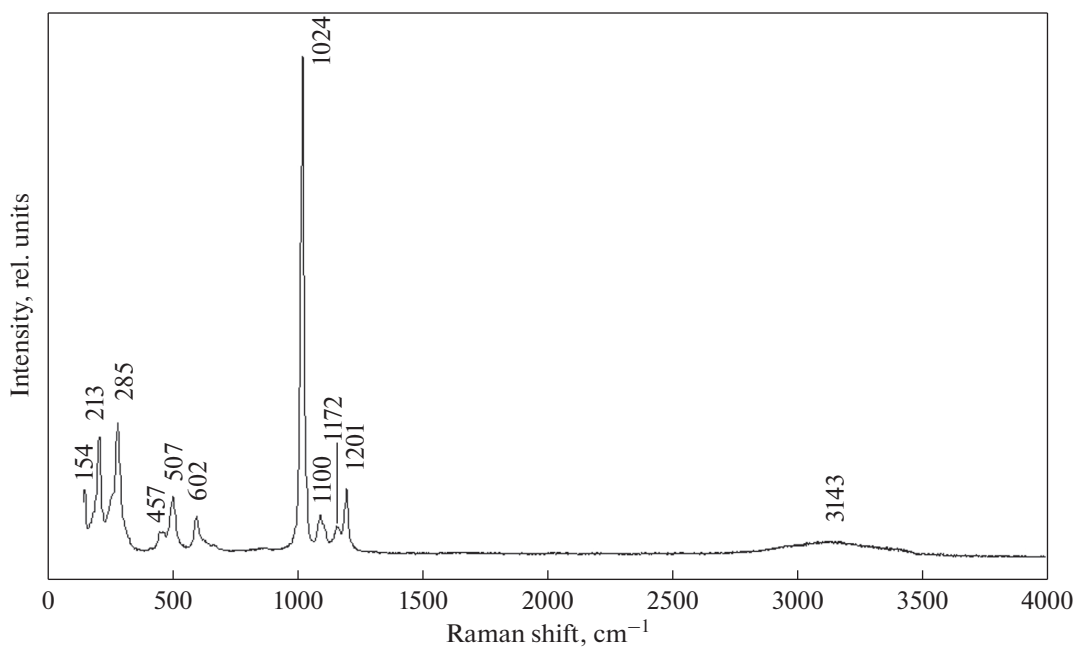
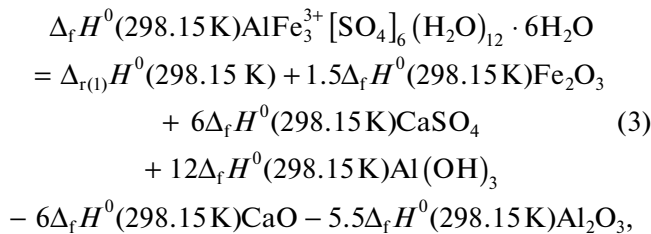


Fig. 4. Raman spectrum of the coquimbite.



where $\Delta H = [H^0(973\text{ K}) - H^0(298.15\text{ K}) + \Delta_{\text{dissol}} H^0(973\text{ K})]$ is thermochemical data for all components involved in reaction (1) (Table 1); $\Delta_f H^0(298.15\text{ K})$ is the enthalpy of formation of the oxides, Al hydroxide, and Ca sulfate (Table 1). The value obtained for the enthalpy of formation of coquimbite $\text{AlFe}_3^{3+} [\text{SO}_4]_6 (\text{H}_2\text{O})_{12} \cdot 6\text{H}_2\text{O}$ from elements is presented in Table 2.

Calorimetric data on the dissolution of natural coquimbite sample allowed us to calculate the enthalpy of formation of aluminocoquimbite $\text{Al}_2\text{Fe}_3^{3+} [\text{SO}_4]_6 (\text{H}_2\text{O})_{12} \cdot 6\text{H}_2\text{O}$ from elements. The experimental values of $[H^0(973\text{ K}) - H^0(298.15\text{ K}) + \Delta_{\text{dissol}} H^0(973\text{ K})]$ were recalculated to the composition of aluminocoquimbite by introducing corrections for the difference between its composition and that of coquimbite, and with regard to the molecular weight. The results of these calculations, which were conducted by equations analogous to (1), (2), and (3), are presented in Table 2.

Gibbs Energy of Formation from Elements

The absolute entropy values needed to calculate the Gibbs energy were calculated as average values for

Table 1. Thermochemical data used to calculate the enthalpy (kJ/mol) of coquimbite and aluminocoquimbite formation

Component	$H^0(973\text{ K}) - H^0(298.15\text{ K}) + \Delta_{\text{dissol}} H^0(973\text{ K})$	$-\Delta_f H^0(298.15\text{ K})^a$
Fe_2O_3 (hematite)	171.6 ± 1.9^b	826.2 ± 1.3
Al_2O_3 (corundum)	107.38 ± 0.59^c	1675.7 ± 1.3
CaO(c)	-21.78 ± 0.29^d	635.1 ± 0.9
CaSO_4 (anhydrite)	131.3 ± 1.6^e	1434.4 ± 4.2
Al(OH)_3 (gibbsite)	172.6 ± 1.9^f	1293.1 ± 1.2

^a Published tabulated data from (Robie and Hemingway, 1995).

^{b–e} Calculated using tabulated data on $[H^0(973\text{ K}) - H^0(298.15\text{ K})]$ (Robie and Hemingway, 1995) and experimental data on dissolution $\Delta_{\text{dissol}} H^0(973\text{ K})$: ^b (Kiseleva, 1976), ^c (Ogorodova et al., 2003), ^d (Kiseleva et al., 1979), ^e (Kotel'nikov et al., 2000).

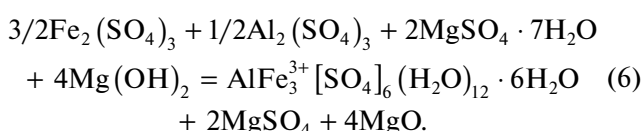
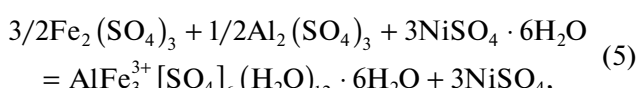
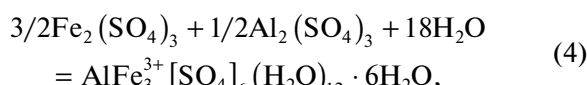
^f According to (Ogorodova et al., 2011).

Table 2. Thermodynamic properties of coquimbite and aluminocoquimbite obtained in this work

Composition and molecular weight, g/mol	$-\Delta_f H^0(298.15 \text{ K})^a$, kJ/mol	$S^0(298.15 \text{ K})^b$, J/(mol K)	$-\Delta_f S^0(298.15 \text{ K})^c$, J/(mol K)	$-\Delta_f G^0(298.15 \text{ K})^d$, kJ/mol
Coquimbite				
$\text{AlFe}_3^{3+} [\text{SO}_4]_6(\text{H}_2\text{O})_{12} \cdot 6\text{H}_2\text{O}$ $M = 1095.18$	11118 ± 40^e	1248.3 ± 3.0	5714.0 ± 3.0	9411 ± 40
Aluminocoquimbite				
$\text{Al}_2\text{Fe}_2^{3+} [\text{SO}_4]_6(\text{H}_2\text{O})_{12} \cdot 6\text{H}_2\text{O}$ $M = 1066.31$	11537 ± 41^f 11543 ± 41^g Average: 11540 ± 29	1226.6 ± 2.9	5736.9 ± 2.9	9830 ± 29

^a According to data of melt solution calorimetry.^b Calculated according to the additivity principle (reactions 4, 5, and 6).^c Calculated using data on $S^0(298.15 \text{ K})$ of elements composing the minerals (Robie and Hemingway, 1995).^d Calculated by the formula $\Delta_f G^0 = \Delta_f H^0 - T\Delta_f S^0$.^e The errors of all thermodynamic values were calculated by the error propagation technique.^f Calculated with regard to M .^g Calculated with regard to the differences in composition.

reactions (4), (5), and (6) for the studied coquimbite and analogous reactions for aluminocoquimbite, using published tabulated data on $S^0(298.15 \text{ K})$ for components of reactions from (Robie and Hemingway, 1995); the contribution of H_2O was assumed to be $39.3 \text{ J}/(\text{mol}\cdot\text{K})$ according to (Naumov et al., 1971).



The values of $\Delta_f S^0(298.15 \text{ K})$ of the minerals (Table 2) were calculated using data on $S^0(298.15 \text{ K})$ of elements of which these minerals consist (Robie and Hemingway, 1995). The values of $\Delta_f G^0(298.15 \text{ K})$ calculated with the use of the data on the entropy and enthalpy of formation are presented in Table 2.

CONCLUSIONS

The thermodynamic data obtained for coquimbite and aluminocoquimbite can be utilized in modeling the weathering of rocks that gives rise to acidic drainage waters at sulfide-bearing ore deposits. The modeling results can also be useful when process flow scenarios are developed for the recovery of valuable components from acidic drainage solutions and for the evaluation of ecological consequences of acidic drainage, designing measures for minimizing adverse envi-

ronmental effects of acidic waters and means for neutralizing and purifying waters of toxic ions of metals.

CONFLICT OF INTEREST

The authors declare that they have no conflicts of interest.

FUNDING

The thermal equipment and mass spectrometer are installed at and belong to the Chemical Faculty of Lomonosov Moscow State University, and the diffractometer, scanning electron microscope, Raman microscope, and Calvet microcalorimeter are installed at and belong to the Geological Faculty of Lomonosov Moscow State University.

REFERENCES

- S. Ackermann, B. Lazic, T. Armbruster, S. Doyle, K.-D. Grevel, and J. Majzlan, “Thermodynamic and crystallographic properties of kornelite $[\text{Fe}_2(\text{SO}_4)_3 \sim 7.75\text{H}_2\text{O}]$ and paracoquimbite $[\text{Fe}_2(\text{SO}_4)_3 \cdot 9\text{H}_2\text{O}]$,” Am. Mineral. **94**, 1620–1628 (2009).
- S. K. Dedushenko and Yu. D. Perfiliev, “On the correlation of the ^{57}Fe Mössbauer isomer shift and some structural parameters of a substance,” Hyperfine Inter. **243**, # 15 (2022).
- F. Demartin, C. Castellano, C. A. Gramaccioli, and I. Campostrini, “Aluminum-for-iron substitution, hydrogen bonding, and a novel structure-type in coquimbite-like minerals,” Can. Mineral. **48**, 323–333 (2010a).
- F. Demartin, C. Castellano, C. A. Gramaccioli, and I. Campostrini, “Aluminocoquimbite, $\text{AlFe}(\text{SO}_4)_3 \cdot 9\text{H}_2\text{O}$, a new aluminum iron sulfate from Grotta Dell'allume, Vulcano, Aeolian Islands, Italy,” Can. Mineral. **48**, 1465–1468 (2010b).

- M. D. Dyar, E. R. Jawin, E. Breves, G. Marchand, M. Nelms, M. D. Lane, S. A. Mertzman, D. L. Bish, and J. L. Bishop, "Mössbauer parameters of iron in phosphate minerals: Implications for interpretation of Martian data," *Am. Mineral.* **99**, 914–942 (2014).
- J. H. Fang and P. D. Robinson, "Crystal structure and mineral chemistry of hydrated ferric sulfates. I. The crystal structure of coquimbite," *Am. Mineral.* **55**, 1534–1540 (1970).
- R. L. Frost, Ž. Ž. Gobac, A. López, Y. Xi, R. Scholz, C. Laná, and R. M. F. Lima, "Characterization of the sulphate mineral coquimbite, a secondary iron sulphate from Javier Ortega mine, Lucanas Province, Peru – Using infrared, Raman spectroscopy and thermogravimetry," *J. Mol. Struct.*, No. 1063, 251–258 (2014).
- B. Hemingway, R. R. Seal, and Chou I. -M. II, "Thermodynamic data for modeling acid mine drainage problems: Compilation and estimation of data for selected soluble iron-sulfate minerals," U.S. Geol. Surv, Open-File Rept. 02–161, (2002).
- IMA List of Minerals. [http://cnnmnc.main.jp/IMA_Master_List_\(2021-11\).pdf](http://cnnmnc.main.jp/IMA_Master_List_(2021-11).pdf).
- I. A. Kiseleva, "Thermodynamic properties and stability of pyrope," *Geokhimiya*, No. 6, 845–854 (1976).
- I. A. Kiseleva, L. P. Ogorodova, N. D. Topor, and O. G. Chigareva, "Thermochemical studies of the CaO–MgO–SiO₂ System," *Geokhimiya*, No. 12, 1811–1825 (1979).
- A. R. Kotel'nikov, Yu. K. Kabalov, T. N. Zezulya, L. V. Mel'chakova, and L. P. Ogorodova, "Experimental study of celestine-barite solid solution," *Geochem. Int.*, No. 12, 1181–1187 (2000).
- J. Majzlan, C. N. Alpers, C. B. Koch, R. B. McCleskey, S. C. B. Myneni, and J. M. Neil, "Vibrational, X-ray absorption, and Mössbauer spectra of sulfate minerals from the weathered massive sulfide deposit at Iron Mountain, California," *Chem. Geol.* **284**, 296–305 (2011).
- J. Majzlan, T. Dordević, and U. Kolitsch, "Hydrogen bonding in coquimbite, nominally Fe₂(SO₄)₃·9H₂O, and the relationship between coquimbite and paracoquimbite," *Miner. Petrol.* **100**, 241–248 (2010).
- J. Majzlan, A. Navrotsky, R. B. McCleskey, and C. N. Alpers, "Thermodynamic properties and crystal structure refinement of ferricopiapite, coquimbite, rhomboclase, and Fe₂(SO₄)₃(H₂O)₅," *Eur. J. Mineral.* **18** (2), 175–186 (2006).
- D. Mauro, C. Biagioli, M. Pasero, H. Skogby, and F. Zaccarini, "Redefinition of coquimbite, AlFe₃(SO₄)₆(H₂O)₁₂·6H₂O," *Mineral. Mag.* **84**, 275–282 (2020).
- G. B. Naumov, B. N. Ryzhenko, and I. L. Khodakovskiy, *A Reference Book of Thermodynamic Values (for Geologists)* (Atomizdat, Moscow, 1971) [in Russian].
- L. P. Ogorodova, I. A. Kiseleva, L. V. Melchakova, M. F. Vigasina, and E. M. Spiridonov, "Calorimetric Determination of the Enthalpy of Formation for Pyrophyllite," *Russ. J. Phys. Chem. A* **85** (9), 1609–1611 (2011).
- L. P. Ogorodova, L. V. Melchakova, I. A. Kiseleva, and I. A. Belitsky, "Thermochemical study of natural pollucite," *Thermochim. Acta* **403**, 251–256 (2003).
- J. T. Poitras, E. A. Cloutis, M. R. Salvatore, S. A. Mertzman, D. M. Applin, and P. Mann, "Mars analog minerals' spectral reflectance characteristics under Martian surface conditions," *Icarus* **306**, 50–73 (2018).
- R. A. Robie and B. S. Hemingway, "Thermodynamic properties of minerals and related substances at 298.15 K and 1 bar (105 pascals) pressure and at higher temperatures," *US Geol. Surv. Bull.*, No. 2131, (1995).
- P. D. Robinson and J. H. Fang, "Crystal structure and mineral chemistry of hydrated ferric sulfates. II. The crystal structure of paracoquimbite," *Am. Mineral.* **56**, 1567–1572 (1971).
- N. Turenne, A. Parkinson, D. M. Applin, P. Mann, E. A. Cloutis, and S. A. Mertzman, "Spectral reflectance properties of minerals exposed to Martian surface conditions: Implications for spectroscopy-based mineral detection on Mars," *Planet. Space Sci.* **210**, 105377 (2022).
- Z. Yang and G. Giester, "Structure refinement of coquimbite and paracoquimbite from the Hongshan Cu–Au deposit, NW China," *Eur. J. Mineral.* **30**, 849–858 (2018).

Translated by E. Kurdyukov